Carbohydrate Polymers 81 (2010) 700–706

Contents lists available at ScienceDirect

Carbohydrate Polymers

journal homepage: www.elsevier.com/locate/carbpol

Characteristic physicochemical features of the biopolymer inulin in solvent added and depleted states

Bappaditya Naskar, Abhijit Dan, Soumen Ghosh, Satya P. Moulik*

Centre for Surface Science, Department of Chemistry, Jadavpur University, Kolkata 700032, India

ARTICLE INFO

Article history:
Received 4 February 2010
Received in revised form 13 March 2010
Accepted 23 March 2010
Available online 31 March 2010

Keywords:
Inulin
Viscosity
Configuration
Morphology
Solubility
Aquo-DMSO
Aquo-IP

ABSTRACT

The β (2 → 1) fructosyl fructose unit containing carbohydrate polymer (inulin) exhibits interesting solution properties. Its physicochemical behaviors in aqueous and aquo-organic (DMSO–water and isopropanol (IP)-water) media as well as in solvent depleted states have been investigated using viscometry, DLS, TEM and AFM methods. The solvent type and composition dependent changes in aggregation of the biopolymer have been examined. The energetics of solubility of inulin in water and IP-water media, and the salt effect on the process have been evaluated. The salting out phenomenon has been examined in terms of Hofmeister or lyotropic series. Its correlation with ionic radius, hydrodynamic radius, and lyotropic number has been tested. The molecular configurations of the polysaccharide in the solvent media have been assessed by the DLS method. In the solvent removed state, globular, rod-like and elongated fiber-like species registering fingerprint patterns of the biopolymer have been witnessed from TEM and AFM measurements.

1. Introduction

The biopolymer inulin has many uses and applications (Ali, Bolton, & Gaylord, 1991; Carswell, O'Rear, & Grady, 2003; Chavanpatil et al., 2007; Griffiths et al., 2007; Kapoor & Chauhan, 2008; Somasundaran & Cleverdon, 1985). It is a fat replacer, a colon and mammary tumor inhibitor and favorable diabetic food ingredient. This β (2 → 1) fructosyl fructose unit containing polydisperse polysaccharide (schematically depicted in our earlier study, Dan, Ghosh, & Moulik, 2009) can promote growth of intestinal bacteria, and increase absorption of both calcium and magnesium. It is a reserved plant polysaccharide (Prazinik, Beck, & Nitsch, 1984; Van loo, Conssement, De Leenher, Hoebregs, & Smits, 1995) which can be synthesized, *in vitro* (Stevens, Meriggi, & Booten, 2001; Wada, Sugatani, Terada, Ohguchi, and Miwa, 2005). The chief sources of inulin are in the plant, chicory, dahlia and Jerusalem artichoke. Electron and X-ray powder diffraction studies have revealed orthorhombic (Andre et al., 1996) and pseudohexagonal (Andre, Putaux, Chanzy, Taravel, Timmermans, & de Wit, 1996) geometries for the hydrated and semi-hydrated inulin, respectively. The polymer has been characterized in both solid state and in solution (Rusu, Bandur, Manoviciu, Rusnac & Plesu, 2006; Stevens et al., 2001b). Its molar mass and solution viscosity in several solvents have been measured (Azis, Chin, Deacon, Harding, & Pavlov, 1999; Bouchard, Hofland, and Witkamp, 2007). But studies on different solution properties of inulin remain to be inadequate. Recently, we have attempted to characterize chicory inulin in both solid and solution states. Its molar mass, sorption of water vapor, thermal solubility, hydration, viscosity behavior in water and in DMSO, molecular association and configuration in these media, etc have been studied (Dan et al., 2009). The polymer has evidenced interesting solution behavior which has prompted us to study the polymer further.

Binary combinations of solvents viz, DMSO–water and IP-water have been used in this study. DMSO is a dipolar aprotic solvent whereas IP is moderately polar and protic. Both are important solvents in chemistry, biochemistry, pharmacy and medicine for dissolution of various substances. The former is an antifreezing agent, and can strongly interact with water. IP is a disinfecting liquid, and is used in pharmaceutical purposes. We are herein interested on the physicochemical behaviors of the biopolymer inulin in mixed solvents of both DMSO and IP with water, and have planned to make a detailed investigation on the solution properties of inulin. The results have been comprehensively presented and discussed from physicochemical view points.

2. Experimental

2.1. Materials

The herein used inulin (extracted from chicory) was a 99% pure product of Sigma (USA). Its weight average molar mass determined by static light scattering method was 4468 g mol^{-1}. Inulin isolated

* Corresponding author. Fax: +91 33 2414 6266.
E-mail address: spmcss@yahoo.com (S.P. Moulik).

0144-8617/$ – see front matter © 2010 Elsevier Ltd. All rights reserved.
doi:10.1016/j.carbpol.2010.03.041

from natural sources range between 4000 and 6500 g mol^{-1}. The AR grade salts used were LiCl, NaCl, KCl, NH_4Cl, Na_3PO_4, $NaNO_3$, Na_2SO_3 (Merck, India), $MgCl_2$, CsCl, NaBr, NaI (SRL, India), and $CuCl_2$, $CaCl_2$, $BaCl_2$, $CdCl_2$, $HgCl_2$, Na_2SO_4, $MgSO_4$, K_2SO_4, $CuSO_4$ (Loba, India). The DMSO and isopropanol were also AR grade quality materials from Merck (Germany) and SRL (India), respectively. These materials were used as received. The concentration of the desiccated inulin used has been expressed in weight percent throughout the text. Doubly distilled water (specific conductance, κ = 2–3 μs cm^{-1} at 30 °C) was employed for preparation of all solutions.

2.2. Viscometry

An Ubbelohde viscometer of 190.4 s average flow time for 13 mL water at 30 °C was used in the study. It was placed in a thermostated water bath of accuracy ±0.1. The flow time of a solution in the viscometer was taken after thermal equilibrium allowing 15 min time for each solution prior to measurement. The standard deviations of the measured viscosities were within ±0.5%. Each measurement was duplicated, and the mean value was recorded and used.

2.3. Solubility

The solubility experiments (i.e. point of turbidity) were performed visually in an illuminated condition in a thermostated water bath. In actual experiment, isopropanol was progressively added with a Hamilton microsyringe into 2 mL aqueous inulin solution at varied concentrations at different temperatures. In another experiment, desired concentrated salt solution was added into 2 mL of 0.01 g g^{-1} inulin solution in IP-water medium at mole fraction of X_{IP} = 0.016 at 30 °C. The point of turbidity was detected by comparing with the pure inulin solution against an illuminated background.

2.4. Dynamic light scattering (DLS)

DLS measurements were taken at 90° angle in a Malvern Zetasizers Nano-zs apparatus with a He–Ne laser (λ = 632 nm) at 25 °C. The sample cells were placed in a temperature-controlled, refractive index matched bath filled with cis-trans decahydronaphthalene (decalin). All experimented solutions were filtered 3–4 times through membrane filters (porosity 0.25 μ) to remove dust particles. The mean values of duplicated experiments are reported.

2.5. Transmission electron microscopy (TEM)

The TEM measurements on inulin were taken with a JEOL JEM 2010 (Tokyo, Japan) high resolution transmission electron microscope (HRTEM) operating at 200 kV. For preparing the TEM sample a drop of the desired solution was placed onto the carbon-coated copper grid giving some time for spreading. It was subjected to slow drying under vacuum. Under such a condition morphological changes of the sample was considered minimal.

2.6. Atomic force microscopy (AFM)

The topological images of the inulin samples taken on glass slides were taken with a Nanosurf Easy Scan2 (Ruschlikon, Switzerland) AFM in contact mode with a constant force of 20 mN. A drop of the inulin solution was placed onto the glass surface, and it was dried by slow heating followed by cooling.

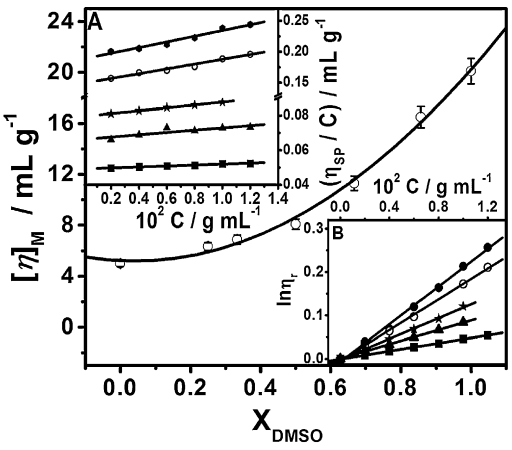

Fig. 1. Dependence of $[\eta]_M$ on X_{DMSO} at 30 °C. Inset A: Huggins plot of $[\eta]_{sp}/C$ vs C at 30 °C. Inset B: Kraemer's plot of ln η_r vs C at 30 °C. (●) DMSO; (○) 6:1 (DMSO:water); (⋆) 1:1 (DMSO:water); (▲) 1:2 (DMSO:water); (■) water. Solvent compositions are in mole ratio.

3. Results and discussion

3.1. Characteristics of inulin solution

3.1.1. Viscosity in DMSO–water and IP-water media

The intrinsic viscosities $[\eta]$ of inulin solutions in water and DMSO media have been reported earlier (Dan et al., 2009). The polymer was found to form globular aggregates in aqueous medium and rod-like assembles in DMSO with appreciable difference in the $[\eta]$ values. We have herein studied the viscosity behavior of the biopolymer in mixed DMSO–water and IP-water media to examine changes in the aggregate morphology, if any. Fig. 1 depicts the observations in DMSO–water medium. The plots in terms of Huggins Eq. (1) have shown fair changes in the intrinsic viscosity by Huggins rationale $[\eta]_H$ (the intercept); the changes in Huggins constant, k_H (derived from the slope) were only moderate. The values are presented in Table 1. The $[\eta]_H$ increases with increasing [DMSO]. Excepting X_{DMSO} = 0.25, the k_H values at other [DMSO] were close; the average value $(k_H)_{ave}$ was found to be 1.44 ± 0.42.

$$\frac{\eta_{sp}}{C} = [\eta]_H + k_H[\eta]_H^2 C \quad (1)$$

where η_{sp} is the specific viscosity of the polymer solution [$\eta_{sp} = \eta_r$ (relative viscosity) − 1], and C is the solute concentration in g mL^{-1}; the other terms are already defined.

The Huggins plots at different DMSO content in the medium are presented in Fig. 1, inset A. The increasing DMSO content increased $[\eta]_H$ i.e., the globular geometry of the polymer aggregates changed to elongated form ultimately to produce rod-like supra aggregates in pure DMSO medium (Dan et al., 2009).

The configuration of the $[\eta]_H$ by Huggins equation was checked by examining the results in the light of the Kraemer's Eq. (2) in the following form (Kraemer, 1938; Sornsrivichiani, 1986 cited by

Table 1
Dependence of $[\eta]^a$ and $k_H{}^a$ on the solvent composition at 30 °C.

X_{DMSO}	$[\eta]_H$/mL g^{-1} ($[\eta]_K$/mL g^{-1})	$[\eta]_M$/mL g^{-1}	k_H
0	4.40 (4.37)	4.38	1.05
0.25	5.86 (6.8)	6.33	2.12
0.33	6.63 (7.11)	6.87	1.50
0.50	7.96 (8.17)	8.08	1.27
0.67	11.0 (11.6)	11.3	1.09
0.86	14.9 (18.1)	16.5	1.75
1.0	18.8 (21.4)	20.1	1.30

[a] Errors in $[\eta]$, and k_H were ±5, and ±10%, respectively on the average.

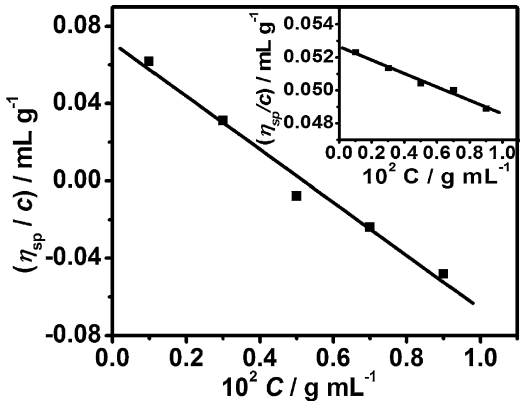

Fig. 2. Huggins plot of $[\eta]_{sp}$/C vs C at X_{IP} = 0.032 for inulin at 30 °C. Inset: same plot at X_{IP} = 0.016.

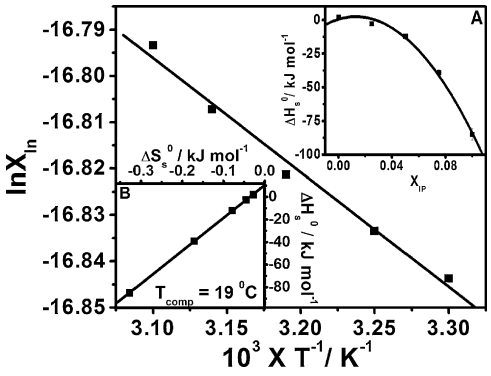

Fig. 3. Plot of ln X_{In} vs T^{-1} in aqueous medium. Correlation coefficient = 0.994. Inset A: profile of ΔH_S° vs X_{IP}. Correlation coefficient = 0.995. Inset B: compensation plot of ΔH_S° vs ΔS_S° for the solubalization process at 30 °C. Correlation coefficient = 0.999.

Higiro, Alavi, & Benn, 2007). The experimental results fitted well with the equation.

$$\ln\ \eta_r = [\eta]_K C \tag{2}$$

where $[\eta]_K$ is the intrinsic viscosity by Kraemer's equation.

The Kraemer's plots for inulin in DMSO–water medium are illustrated in the inset B, Fig. 1. The $[\eta]_K$ values are also presented with $[\eta]_H$ in Table 1. This restricted form of Kraemer's equation has been also found to obey by different gums in salt solution (Banerjee, Mukherjee, Bhattacharya, Datta, & Moulik, 2009). The $[\eta]_H$ and $[\eta]_K$ were also found to fairly agree. The mean values ($[\eta]_M$) have been taken as the intrinsic viscosities of inulin in water and DMSO–water media. The $[\eta]_M$ increased exponentially with DMSO content (Fig. 1, main plot). The following relation (correlation coefficient = 0.995) was found to describe the results.

$$[\eta]_M = A + B[X_{DMSO}] + C[X_{DMSO}]^2 \tag{3}$$

where A, B, and C are the polynomial constants (A = 4.68; B = 0.006; C = 0.002).

The addition of IP in water significantly affected the solubility of inulin; the solubility decreased with increasing IP concentration. At X_{IP} = 0.032, the solubility decrease was perceptible. Two IP-water compositions of X_{IP} = 0.016 and 0.032 were used in the study. Fig. 2 depicts the Huggins plot that showed a marked distinction from DMSO–water medium. Interestingly, the plots evidenced negative slopes which are only rarely found. The $[\eta]_H$ values at X_{IP} = 0.016 and 0.032 were 5.25 and 7.13 mL g^{-1}, respectively. The results suggested changing geometry of inulin from globular to non-globular form in the presence of IP in water as observed for DMSO–water medium. The negative values were unusual and exceptional. From literature survey, we have found such a behavior for the protein lysozyme (Kamiyama, Morita, & Kimura, 2004) where also $[\eta]_H$ increased with increasing [DMSO] yielding negative k_H values. DMSO denatured lysozyme making it elongated with increasing $[\eta]$. The negative k_H arose because of decline in the rate of increase of η_{sp} per unit concentration of lysozyme. In the present context, it was a consequence of the effect of solute on the solvent fluidity which increased to make η_{sp}/C decline with [inulin] in the IP-water medium. More elaborate studies of the system need to be executed in future under varied environmental conditions for further elucidation of this uncommon observation. We may herein add that in a recent study (Yilgor, Ward, Yilgor, & Atilla, 2006) negative k_H values have been found from the viscosity measurements of segmented polydimethylsiloxane–polyurea copolymers in IP medium. Exceptionally strong polymer solvent interactions leading to conformational transitions have been considered for such a behavior.

3.1.2. Solubility in IP-water medium

The solubility of inulin in water (~0.10 g g^{-1}) at 30 °C was found to decrease by the addition of IP. For instance at X_{IP} = 0.032, the solubility became 1/10th of that without IP. The effect was studied at five different temperatures 30, 35, 40, 45 and 50 °C, and energetics of the process were evaluated at X_{IP} = 0, 0.025, 0.05, 0.075, and 0.1. The ln(solubility) vs X_{IP} profiles (not illustrated) at the above mention temperatures were fairly linear with correlation coefficient of 0.994, 0.996, 0.996, 0.992 and 0.994, respectively. The data were processed in the light of the integrated van't Hoff Eq. (4) to calculate the standard enthalpy of solution (ΔH_S°).

$$\ln X_{In} = I - \frac{\Delta H_S^\circ}{RT} \tag{4}$$

where X_{In} is the solubility of inulin expressed in mole fraction unit, I is the intercept, R is the gas constant, and T is the absolute temperature.

Fig. 3 (main plot) represents the van't Hoff plot to derive ΔH_S° from the slope. The estimated ΔH_S° values at different X_{IP} in water are graphically presented in the inset A of Fig. 3. The ΔH_S° in water was weakly endothermic and became more and more exothermic by the increasing presence of IP in solution. The exothermicity rapidly increased with increasing X_{IP}. The $\Delta H_S^\circ - X_{IP}$ profile fitted to a polynomial equation of the following form,

$$\Delta H_S^\circ = a + bX_{IP} + cX_{IP}^2 \tag{5}$$

where a, b, and c are the polynomial constants (a = 0.49; b = 298.3; c = −11402).

We may mention here that although there are not enough points to make the plot statistically significant, the procedure has yielded a fair correlation (correlation coefficient = 0.995). Such a plot, we believe is better than any other arbitrary plots of the experimental results. The correlation of the other two plots in Fig. 3 is also given in the legend. They are comparable with the plot in inset B.

In the experiment, the appearance of stable point of turbidity was taken as the point of solubility. The corresponding standard free energy of solution was obtained from a relation,

$$\Delta G_S^\circ = -RT \ln X_{In} \tag{6}$$

ΔS_S° (standard entropy of solution) was calculated by combining Eqs. (4) and (6) what is known as the Gibbs-Helmholtz relation,

$$\Delta S_S^\circ = \frac{\Delta H_S^\circ - \Delta G_S^\circ}{T} \tag{7}$$

The calculated energetic values at 30 °C are herein presented against X_{IP} in the sequence, ΔH_S°, ΔG_S° and ΔS_S°. Thus, at X_{IP} = 0, the values are 2.06, 10.5 and 27.8; X_{IP} = 0.025, they are −2.65, 11.0 and 45.0; at X_{IP} = 0.05, they are −12.1, 11.7 and 78.5; at X_{IP} = 0.075, they

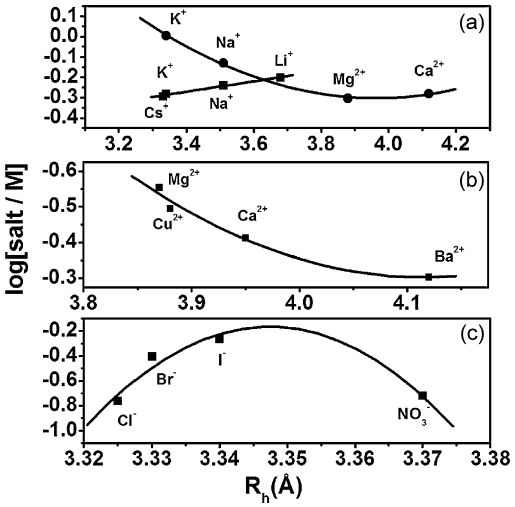

Fig. 4. Dependence of salting out concentration of ions (required to destabilize 0.01 g g^{-1} inulin solution in X_{IP} = 0.016 medium) on hydrodynamic radius (R_h) at 30 °C. (A) cations with common anion Cl^- (■), and SO_4^{2-} (●); (B) cations with common anion Cl^-; and (C) anions with common cation Na^+.

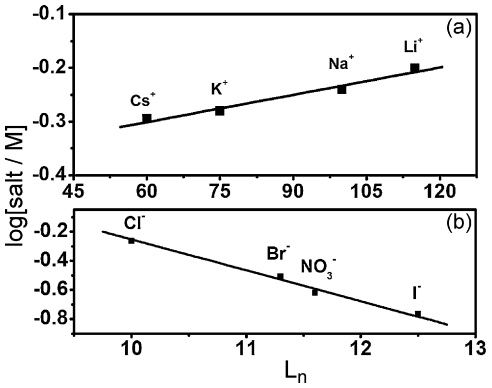

Fig. 5. Dependence of salting out concentration of ions (required to destabilize 0.01 g g^{-1} inulin solution in X_{IP} = 0.016 medium) on the lyotropic number (L_n) at 30 °C. (A) Cations with common anion Cl^- and (B) anions with common cation Na^+.

are −39.1, 12.7 and 171.0; at X_{IP} = 0.1 they are −84.9, 14.2 and 327.0. The ΔH_S° and ΔG_S° are expressed in kJ mol^{-1} whereas the ΔS_S° are expressed in J K^{-1} mol^{-1}. Their relative errors are 5, 3 and 8%. The phase separation process of inulin in IP-water medium was associated with large entropy change. The release of associated solvent from the biopolymer during precipitation from the solution contributed favorably to produce increasing entropy with increased proportion of IP in the medium. The evaluated ΔH_S° and ΔS_S° were found to produce a good compensation correlation (Fig. 3, inset B). The compensation temperature obtained from the slope was 19 °C vis-a-vis the average temperature (40 °C) of the study. The extra thermodynamic compensation temperature evidenced fair deviation from the average temperature which of course is not an uncommon citation in literature (Mukherjee, Mitra, Bhattacharya, & Moulik, 1995; Mukherjee, Mukherjee, & Moulik, 1994; Sugihara, Nakano, Sulthana, & Rakshit, 2001).

3.1.3. Salt effect on solubility in IP-water medium

The salting out of hydrophilic colloids and polymers (Bales & Zana, 2004; Nostro, Fratoni, Ninham, & Baglioni, 2003; Prasad et al., 2005; Saito, 1969; Schott, 1998) from aqueous solution is an important and complex problem in chemistry. The ions of salts are classified in terms of a series (Glasstone, 1960) called 'Lyotropic' or 'Hofmeister Series'. Although salting out of inulin is difficult from aqueous solution, it can be fairly achieved in IP-water medium since the medium fairly decreased inulin solubility as mentioned above. We have studied the salting out of the polysaccharide from IP-water medium at X_{IP} = 0.016 at a fixed polymer concentration (0.01 g g^{-1}) using a large number of inorganic (mono-, bi-, and trivalent) salts. In this study, we have measured the solubility limits of the 0.01 g g^{-1} polymer solution in presence of salts at 30 °C, and a correlation of the results has been attempted. The correlation of results in terms of ionic radius, hydrodynamic radius, and lyotropic number has been attempted. Linear dependences in terms of ionic radius for both cations and anions with common anions and cations, respectively of the salts studied (cf. Section 2.1) were observed (illustration not presented). The trends either increased or decreased for both the series. In comparison with monovalent ions, multivalent ion effects on solubility decrease were greater. Comparative results in terms of hydrodynamic radius (R_h) of ions are illustrated in Fig. 4. The trends varied, the correlations were also less orderly. According to the reported Hofmeister Series (Glasstone, 1960), the salting out effectivity sequence of cations with a common anion (Cl^-) is $Mg^{2+} > Ca^{2+} > Sr^{2+} > Ba^{2+} > Li^+ > Na^+ > K^+ > Rb^+ > Cs^+$ (Mg^{2+} is the strongest and Cs^+ is the weakest). Such sequence for anions with a common cation (Na^+) is $citrate^{3-} > tartarate^{2-} > SO_4^{2-} > PO_4^{3-} > acetate^- > Cl^- > NO_3^- > ClO_3^- > I^- > SCN^-$ ($citrate^{3-}$ is the strongest and SCN^- is the weakest). The orders realized in this study were (1) $Cd^{2+} > Ba^{2+} > Cu^{2+} > Ca^{2+} > Mg^{2+} > NH_4^+ > Cs^+ > K^+ > Na^+ > Li^+$ for cations, and (2) $SO_4^{2-} > PO_4^{3-} > NO_3^- > SCN^- > I^- > Br^- > Cl^-$ for anions.

The observed sequence for inulin insolubility caused by cations on the whole followed a reverse Hofmeister Series (HS) order. It was disorderly for anions. The plot of solubility vs lyotropic number (L_n) available for ions is depicted in Fig. 5, which has produced a good correlation among the studied ions and the monovalent anions (although showed reverse order with reference to HS) resulted a better fitting than the anions. The anomaly of salting out effect on inulin solubility (to produce a reverse HS order) has been also recently observed on critical micellar concentration (CMC) of ionic surfactants, and several other micellar parameters (Maiti, Mitra, Guha, & Moulik, 2009). Why both the systems produced reverse HS order requires rationalization. They represent two different processes from the normal salting out phenomenon of hydrophilic colloids and polymers considered to develop the HS series in aqueous medium. Herein inulin was studied in IP-water medium, and the earlier studied micellization process (surfactant self-aggregation in aqueous salt solution) was basically two different processes. The solvent type (its polarity and type in particular), and the solute type (its dual polar–nonpolar composition as in amphiphiles) should have their say on the effectivity of the HS order. This remains to be analyzed by way of additional studies in this line.

3.2. Morphology in solution and in desolvated states

3.2.1. DLS measurements

In our previous work (Dan et al., 2009), the DLS results for inulin in water evidenced formation of two types of solvated species, the compact monomer ($\overline{R}_h = 16$ nm) and supra aggregates ($\overline{R}_h = 98$ nm), where $\overline{R}_h$ is the average hydrodynamic radius. These results were compared with the non-solvated species of radii 11 and 68 nm, respectively determined from TEM measurements, and the differences were accounted for their solvation. In this study, $\underset{C=0}{\text{Lt}}\,\overline{R}_h$ at X_{DMSO} = 0.50 in DMSO–water medium was found to be 244 nm but the TEM results on the higher side was 80 nm. The difference was large; probably the mixed DMSO–water produced

Table 2
Hydrodynamic radius ($\overline{R}_h^0$)[a,b] and polydispersity index (PDI) of inulin solution in different solvent media at 25 °C.

Medium	$\overline{R}_h^0$/nm	PDI
Water	16 (98)	0.331
DMSO	19 (152)	0.493
X_{DMSO} = 0.50	(244)	0.574
X_{IP} = 0.016	19 (62)	0.484
X_{IP} = 0.032	30 (134)	0.386

[a] The $\overline{R}_h$ values depended on [inulin]. The reported values are concentration independent i.e. $\overline{R}_h^0 \equiv \underset{C=0}{\text{Lt}}\, \overline{R}_h$. Aggregate hydrodynamic radius is in parenthesis.

[b] Errors in $\overline{R}_h^0$, ±12%.

greater solvation. The results in pure DMSO and IP-water media are presented in Table 2. Although the values appeared to be reasonable, their comparison and discussion are less relevant since the DLS method produces results on the basis of spherical geometry of the scattering species which in the present system was not so as revealed from the desolvated TEM pictures to be subsequently discussed. The above results warrant further physicochemical studies of the biopolymer inulin in solution in different mixed solvent media, and in presence of additives.

3.2.2. TEM and AFM studies

The morphology dependence of the solvent removed inulin obtained from DMSO–water medium was examined by TEM and AFM measurements. The TEM images of samples from the mixed DMSO–water medium at X_{DMSO} = 0.50 and 1.0 are illustrated in Fig. 6A and B. Globular supra molecular inulin aggregates formed (Dan et al., 2009) in water that changed to spindle-shaped rod-like aggregates in DMSO, and heterogeneous roughly prolate shaped aggregates of intermediate dimensions appeared from the aforesaid DMSO–water medium. The AFM images in pure DMSO medium (depicted in Fig. 6D and E) witnessed topography of elongated aggregates. The three-dimensional depiction (Fig. 6E) supported pointed tip particles with average surface roughness of ~34 nm in DMSO. Nearly globular topography with much shorter heights were observed for samples prepared from X_{DMSO} = 0.50 mixed medium in their AFM pictures (not illustrated). Thus, solvent composition dependent aggregate formation of the biopolymer inulin in DMSO–water medium was witnessed.

The morphology of inulin obtained from IP-water medium was also studied by TEM and AFM measurements. For both X_{IP} = 0.016 and 0.032 in IP-water medium (Fig. 6C), fingerprint patterned structures were observed. The particles became self-arranged generating elongated fiber-like morphology. The width of the fibers at X_{IP} = 0.016 and 0.032 were on the average 3.1 and 2.3 nm, respectively; and the distances between two layers were 2.8 and 6.2 nm, respectively. Such TEM images are not very commonly observed. In recent literature (Chen, Joly, Malm, Bovin, & Wang, 2003; Cozzoli, Kornowoski, & weller, 2003; de Gennes & Prost, 1993; Nich, Harroun, Raghunathan, Glinka, & Katsaras, 2004; Yu & Saupe, 1980), fingerprint impressions in TEM for polymer, surfactant and polymer-nanoparticle composites have been reported. The samples on the grid form narrow fiber-like bodies that arrange in definite patterns like fingerprints. Khatua, Ghosh, Dey, Ghosh, and Aswal (2008) reported fingerprint like TEM patterns for a mixed surfactant system of sodium N-(2-(*n*-dodecylamino)ethanoyl)-L-alaninate (C_{12}Ala) and sodiumdodecyl sulfate (SDS) in aqueous solution at a molar ratio of 0.2. Fingerprint-like structures forming circular cylinder type pattern was observed from semi dilute solutions. Rod-like micelles transformed into elongated long threads of ~2 nm width to produce the pattern which was recognizable up to a concentration of 10 mM. The presence of chirality in the molecules has been considered to be a necessary condition for this pattern. But achiral compounds have been also found to form such structures (Castaldi, Ortona, Paduano, & Vitagliano, 1998; Sulthana, Rao, Bhat, & Rakshit, 1998). The desolvated inulin from IP-water used in this study was CD (circular dichroism) inactive achiral species (without optical rotation), and has formed fingerprint patterns. Such patterns were not obtained for samples prepared from water and DMSO media (cf. Fig. 6A and B). The nature of the solvent and broadly speaking, the environment has to have a say on such pattern formation. Thus at this stage, generalization would be a premature comprehension. The AFM images at X_{IP} = 0.016 and

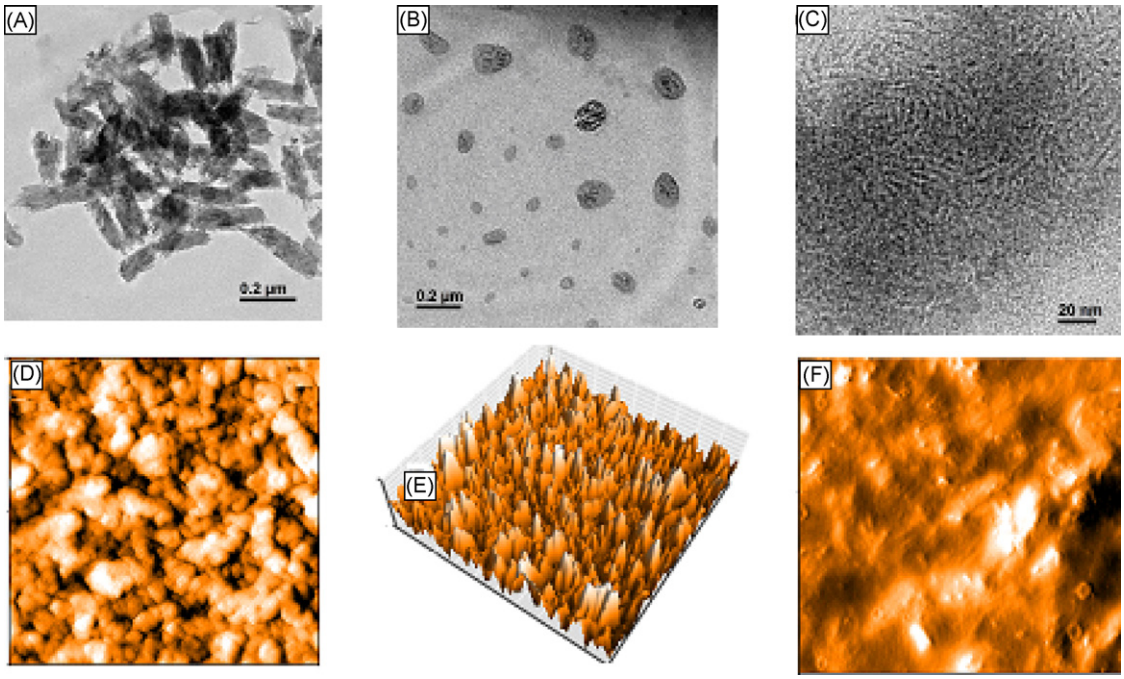

Fig. 6. TEM and AFM images of inulin (0.05 mg g^{-1}) in DMSO–water and IP-water media. (A) TEM in pure DMSO; (B) TEM in X_{DMSO} = 0.50; (C) TEM in X_{IP} = 0.032; (D) AFM in pure DMSO (2D picture, dimension 10/10 μm); (E) AFM in pure DMSO (3D picture, dimension 30/30/0.12 μm); and (F) AFM in X_{IP} = 0.032 (dimension, 50/50 μm).

0.032 in water evidenced kind of elongated topography (Fig. 6F at $X_{IP} = 0.032$). The average surface roughness of the preparation was ~55 nm.

4. Conclusion

The biopolymer forms aggregates in solution; both monomeric and large aggregates have been supported from DLS measurements. Inulin is fairly soluble in water; it is liberally soluble in DMSO but sparingly soluble in IP medium. Its [η] viscosity in water is much smaller than in DMSO, and intermediate in DMSO–water medium increasing continuously with increasing concentration of the first component. The solubility of inulin in water decreases with temperature (hydrophobic effect), and the process is weakly endothermic. In IP-water environment the process becomes distinctly exothermic; the exothermicity increases with increasing presence of IP in the medium. In IP-water environment, the solubility of inulin decreases by the addition of salt. The salting out phenomenon only partially follows the Hofmeister or lyotropic series for the ions. The solubility has shown a moderate correlation with the hydrodynamic radius of the effective ions, and a fair correlation with their lyotropic numbers.

The TEM measurements of solvent removed samples of inulin evidence radical morphology differences. The sample from water produces globular aggregates whereas that from DMSO shows thick spindle-like species. In DMSO–water at $X_{DMSO} = 0.50$, the aggregates are non-spherical. At $X_{IP} = 0.016$ and 0.032 in IP-water medium, the aggregates are also non-spherical, and produce fiber-like assemblies arranged in fingerprint patterns. AFM pictures of these samples have supported the formation of spherical, non-spherical and elongated entities.

Acknowledgements

B.N. and A.D. thank UGC, Government of India, for Junior Research Fellowship and Senior Research Fellowship, respectively to perform this work. Contingency support by Indian National Science Academy to S.P.M. is thankfully acknowledged. The cooperation of Mr. S. Basak and Mr. R. Paul during DLS and AFM experiments at IICB and J.U., respectively has been appreciated.

References

Ali, D., Bolton, S., & Gaylord, N. G. (1991). Hydroxypropylmethylcellulose–anionic surfactant interactions in aqueous systems. *Journal of Applied Polymer Science*, *42*, 947–956.

Andre, I., Mazeau, K., Tvaroska, I., Putaux, J.-L., Winter, W. T., Taravel, F. R., et al. (1996). Molecular and crystal structures of inulin from electron diffraction data. *Macromolecules*, *29*, 4626–4635.

Andre, I., Putaux, J. L., Chanzy, H., Taravel, F. R., Timmermans, J. W., & de Wit, D. (1996). Single crystal of inulin. *International Journal of Biological Macromolecules*, *18*, 195–204.

Azis, B. H., Chin, B., Deacon, M'P., Harding, S. E., & Pavlov, G. (1999). Size and shape of inulin in dimethyl sulphoxide solution. *Carbohydrate Polymers*, *38*, 231–234.

Bales, B. L., & Zana, R. (2004). Cloud point of aqueous solutions of tetrabutylammonium dodecyl sulfate is a function of the concentration of counterions in the aqueous phase. *Langmuir*, *20*, 1579–1581.

Banerjee, P., Mukherjee, I., Bhattacharya, S., Datta, S., & Moulik, S. P. (2009). Sorption of water vapor, hydration, and viscosity of carboxymethylhydroxypropyl guar, diutan and xanthan gums, and their molecular association with and without salts (NaCl, $CaCl_2$, HCOOK, CH_3COONa, $(NH_4)_2SO_4$ and $MgSO_4$) in aqueous solution. *Langmuir*, *25*, 11647–11656.

Bouchard, A., Hofland, G. W., & Witkamp, G.-J. (2007). Properties of sugar, polyol, and polysaccharide water-ethanol solutions. *Journal of Chemical & Engineering Data*, *52*, 1838–1842.

Carswell, A. D. W., O'Rear, E. A., & Grady, B. P. (2003). Adsorbed surfactants as templates for the synthesis of morphologically controlled polyaniline and polypyrrole nanostructures on flat surfaces: From spheres to wires to flat films. *Journal of American Chemical Society*, *125*, 14793–14800.

Castaldi, M. L., Ortona, O., Paduano, L., & Vitagliano, V. (1998). Mutual diffusion measurements in a ternary system: Ionic surfactant–nonionic surfactant–water at 25 °C. *Langmuir*, *14*, 5994–5998.

Chavanpatil, M. D., Khadir, A., Patil, Y., Handa, H., Mao, G., & Panyam, J. (2007). Polymer-surfactant nanoparticles for sustained release of water-soluble drugs. *Journal of Pharmaceutical Science*, *96*, 3379–3389.

Chen, W., Joly, A. G., Malm, J.-O., Bovin, J.-O., & Wang, S. (2003). Full-color emission and temperature dependence of the luminescence in poly-p-phenylene ethynylene-Zns/Mn^{2+} composite particle. *Journal of Physical Chemistry B*, *107*, 6544–6551.

Cozzoli, P. D., Kornowoski, A., & Weller, H. (2003). Low-temperature synthesis of soluble and processable organic-capped anatase TiO_2 nanorods. *Journal of American Chemical Society*, *125*, 14539–14548.

Dan, A., Ghosh, S., & Moulik, S. P. (2009). Physicochemical studies on the biopolymer inulin: A critical evalution of its self-aggregation, aggregate-morphology, interaction with water and thermal stability. *Biopolymers*, *91*, 687–699.

de Gennes, P. G., & Prost, J. (1993). *The physics of liquid crystals*. Oxford, U.K.: Oxford University Press.

Glasstone, S. (1960). *Text book of physical chemistry* (2nd ed.). London: Macmillan., p. 1254.

Griffiths, P. C., Khayat, Z., Tse, S., Heenan, R. K., King, S. M., & Duncan, R. (2007). Studies on the mechanism of interaction of a bioresponsive endosomolytic polyamidoamine with interfaces. 1. Micelles as model surfaces. *Biomacromolecules*, *8*, 1004–1012.

Kamiyama, T., Morita, M., & Kimura, T. (2004). Rheological study of Lysozyme in dimethyl sulfoxide + water solution at 298.15 K. *Journal of Chemical & Engineering Data*, *49*, 1350–1353.

Kapoor, Y., & Chauhan, A. (2008). Drug and surfactant transport in cyclosporine A and Brij 98 laden p-HEMA hydrogels. *Journal of Colloid and Interface Science*, *322*, 624–633.

Khatua, D., Ghosh, S., Dey, J., Ghosh, G., & Aswal, V. K. (2008). Physicochemical properties and microstructure formation of the surfactant mixtures of sodium *N*-(2-(*n*-dodecylamino)ethanoyl-L-alaninate and SDS in aqueous solutions. *Journal of Physical Chemistry B*, *112*, 5374–5380.

Kraemer, E. O. (1938). Molecular weights of celluloses. *Industrial and Engineering Chemistry Research*, *30*, 1200–1203.

Maiti, K., Mitra, D., Guha, S., & Moulik, S. P. (2009). Salt effect on self-aggregation of sodium dodecylsulfate (SDS) and tetradecyltrimethylammonium bromide (TTAB): Physicochemical correlation and assessment in the light of Hofmeister (lyotropic) effect. *Journal of Molecular Liquids*, *146*, 44–51.

Mukherjee, L., Mitra, N., Bhattacharya, B. K., & Moulik, S. P. (1995). Kinetics in microemulsion medium 4. Alkaline fading of crystal violet in aqueous (H_2O/aerosol OT/isooctayl and H_2O/aerosol OT/decane) and nonaqueous (ethylene glycol/aerosol OT/isooctane) microemulsions. *Langmuir*, *11*, 2866–2871.

Mukherjee, K., Mukherjee, D. C., & Moulik, S. P. (1994). Thermodynamics of micellization of aerosol OT in binary mixtures of water, formamide-ethylene glycol and dioxane. *Journal of Physical Chemistry*, *98*, 4713–4718.

Nich, M.-P., Harroun, T. A., Raghunathan, V. A., Glinka, C. J., & Katsaras, J. (2004). Spontaneously formed monodisperse biomimetic unilamellar vesicles: The effect of charge, dilution, and time. *Biophysical Journal*, *86*, 2615–2629.

Nostro, P. L., Fratoni, L., Ninham, B. W., & Baglioni, P. (2003). Water absorbency by wool fibers: Hofmeister effect. *Biomacromolecules*, *3*, 1217–1224.

Prasad, M., Moulik, S. P., Wardian, A. A., Moorse, S., van Bommel, A., & Palepu, R. (2005). Alkyl (C_{10}, C_{12}, C_{14} and C_{16}) triphenyl phosphonium bromide influenced cloud points of nonionic surfactants (Triton X 100, Brij 56 and Brij 97) and the polymer (polyvinyl methyl ether). *Colloid and Polymer Science*, *283*, 887–897.

Prazinik, W., Beck, R. H. F., & Nitsch, E. J. (1984). Determination of fructan oligomers of degree of polymerization 2–30 by high-performance liquid chromatography. *Journal of Chromatography A*, *303*, 417–421.

Rusu, G., Bandur, G., Manoviciu, I., Rusnac, L., & Plesu, N. (2006). Solubility and viscosity studies on inulin modified with methacyloyl and palmitoyl chlorides. *Chemical Bulletin "POLITEHNICA" (Timisoara)*, *51*, 83–86.

Saito, S. (1969). Salt effect on polymer solution. *Journal of Polymer Science Part A-1: Polymer Chemistry*, *7*, 1789–1802.

Schott, H. J. (1998). Comparing the surface chemical properties and the effect of salts on the cloud point of a conventional nonionic surfactant, octoxynol 9 (Triton X-100), and its oligomer, tyloxapol (Triton WR-1339). *Journal of Colloid and Interface Science*, *205*, 496–502.

Somasundaran, P., & Cleverdon, J. (1985). A study of polymer/surfactant interaction at the mineral/solution interface. *Colloids and Surfaces*, *13*, 73–85.

Sornsrivichiani, T. (1986). Ph.D. thesis, Cornell University, Ithaca, NY. Cited by Higiro, J., Alavi, S., & Bean, S. (2007). Rheological study of xanthan and locust bean gum interaction in dilute solution. *Food Research International, 40*, 435–447.

Stevens, C. V., Meriggi, A., & Booten, K. (2001). Chemical modification of inulin, a valuable renewable resource, and its industrial applications. *Biomacromolecules*, *2*, 1–16.

Stevens, C. V., Meriggi, A., Peristeropoulou, M., Christov, P. P., Booten, K., Levecke, B., et al. (2001). Polymeric surfactants based on inulin, a polysaccharide extracted from chicory. 1. Synthesis and interfacial properties. *Biomacromolecules*, *2*, 1256–1259.

Sugihara, G., Nakano, T.-Y., Sulthana, S. B., & Rakshit, A. K. (2001). Enthalpy–entropy compensation rule and the compensation temperature observed in micelle, formation of different surfactants in water. What is the so-called compensation temperature? *Journal of Oleo Science*, *50*, 29–39.

Sulthana, S. B., Rao, P. V. C., Bhat, S. G. T., & Rakshit, A. K. (1998). Interfacial and thermodynamic properties of SDBS–$C_{12}E_{10}$ mixed micelles in aqueous media: Effect of additives. *Journal of Physical Chemistry B*, *102*, 9653–9660.

Van loo, J., Conssement, P., De Leenher, L., Hoebregs, H., & Smits, G. (1995). On the presence of inulin and oligofructose as natural ingredients in the western diet. *Critical Reviews in Food Science and Nutrition*, *35*, 525–552.

Wada, T., Sugatani, J., Terada, E., Ohguchi, M., & Miwa, M. (2005). Physicochemical characterization and biological effects of inulin enzymatically synthesized from sucrose. *Journal of Agricultural and Food Chemistry*, *53*, 1246–1253.

Yilgor, I., Ward, C. T., Yilgor, E., & Atilla, E. G. (2006). Anomalous dilute solution properties of segmented polydimethyl siloxane–polyurea copolymers in isopropyl alcohol. *Polymer*, *47*, 1179–1186.

Yu, L. J., & Saupe, A. (1980). Liquid crystalline phases of the sodium decylsulfate/decanol/water system. Nematic–nematic and cholesteric–cholesteric phase transitions. *Journal of American Chemical Society*, *102*, 4879–4883.